# Stable intronic sequence (sis) RNA, a new class of non-coding RNA from the oocyte nucleus of *Xenopus tropicalis*

Eugene J. Gardner, [1] Zehra F. Nizami, [1] C. Conover Talbot Jr [2] and Joseph G. Gall [1]

[1]Department of Embryology, Carnegie Institution for Science, Baltimore, MD 21218; [2]Institute for Basic Biomedical Sciences, The Johns Hopkins University School of Medicine, Baltimore, MD 21205.

Corresponding author:
Joseph G. Gall
Department of Embryology
Carnegie Institution for Science
3520 San Martin Drive
Baltimore, MD 21218
Phone: (410) 246-3017
e-mail: gall@ciwemb.edu

Running Title: Stable intronic sequence (sis) RNA

Key words: intron; lampbrush chromosome; non-coding RNA; oocyte; transcription; *Xenopus*.

Abbreviations: FPKM, fragments per kilobase per million reads; GV, germinal vesicle; RNAseq, high-throughput RNA sequencing; rRNA, ribosomal RNA; RT-PCR, reverse transcription polymerase chain reaction; sis, stable intronic sequence; UTR, untranslated region

**Abstract**

To compare nuclear and cytoplasmic RNA from a single cell type, free of cross-contamination, we studied the oocyte of the frog *Xenopus tropicalis*, a giant cell with an equally giant nucleus. We isolated RNA from manually dissected nuclei and cytoplasm of mature oocytes and subjected it to deep sequencing. Cytoplasmic mRNA consisted primarily of spliced exons derived from approximately 6700 annotated genes. Nearly all of these genes were represented in the nucleus by intronic sequences. However, unspliced nascent transcripts were not detected. Inhibition of transcription or splicing for 1-2 days had little or no effect on the abundance of nuclear intronic sequences, demonstrating that they are unusually stable. RT-PCR analysis showed that these stable intronic sequences are transcribed from the coding strand and that a given intron can be processed into more than one molecule. Stable intronic sequence RNA (sisRNA) from the oocyte nucleus constitutes a new class of non-coding RNA. sisRNA is detectable by RT-PCR in samples of total RNA from embryos up to the mid-blastula stage, when zygotic transcription begins. Storage of sisRNA in the oocyte nucleus and its transmission to the developing embryo suggests that it may play important regulatory roles during oogenesis and/or early embryogenesis.

**Introduction**

The majority of genes in higher eukaryotes have one or more introns interspersed within the coding region. Either during transcription or shortly afterwards the intronic sequences are removed from the transcript by the splicing machinery (Wahl et al. 2009; Oesterreich et al. 2010; Vargas et al. 2011; Hoskins and Moore 2012). The majority of spliced RNAs are rapidly transported to the cytoplasm, whereas the introns are degraded while still in the nucleus. The primary intronic product of splicing is an intron lariat, in which the 5' end of the intron is covalently linked to the splice acceptor site, an A near the 3' end of the intron. The lariat can be converted to a linear molecule by the debranching enzyme (dbr) (Ruskin and Green 1985). Intron degradation can be a rapid process, requiring only seconds or minutes in the case of yeast and cultured cells (Sharp et al. 1987; Clement et al. 1999; Oesterreich et al. 2010). Much less is known about the lifetime of introns in tissues. A few cases of stable introns have been described (Michaeli et al. 1988; Kopczynski and Muskavitch 1992; Qian et al. 1992; Yang et al. 2011), although it is generally believed that most introns or intron fragments are unstable. There are some exceptions, notably the small nucleolar (sno) RNAs, which are derived by debranching of spliced lariats followed by trimming to produce the mature molecule (Ooi et al. 1998; Petfalski et al. 1998).

In this study we examined RNA derived from oocytes of the frog *Xenopus tropicalis*. We isolated RNA from manually dissected cytoplasmic and nuclear fractions and subjected it to deep sequencing. Cytoplasmic mRNA consists primarily of spliced exons, as expected. Surprisingly, the major nuclear RNA derived from these same genes consists of stable introns or intron fragments. At the read depth of our

experiments, we do not see reads that cross intron-exon boundaries, as would be expected for nascent transcripts. The stable intronic sequences are transmitted to the embryo and persist until at least the blastula stage, when zygotic transcription first begins. We discuss these findings in relation to the special features of RNA transcription and storage in the growing oocyte and early embryo.

**Results**

*Pure cytoplasmic and nuclear RNA can be prepared from Xenopus oocytes*

Amphibian oocytes offer a unique opportunity to analyze nuclear and cytoplasmic RNA fractions with minimal cross-contamination. It is well known that the majority of cytoplasmic RNA consists of the large and small ribosomal RNA (rRNA) subunits and that much of the mRNA consists of stored polyadenylated sequences not associated with polysomes (Radford et al. 2008; Richter and Lasko 2011; earlier studies reviewed in Davidson, 1986). However, the nature of nuclear RNA has not been systematically investigated. *Xenopus laevis* was the favored species for earlier studies on RNA, but *X. tropicalis* has the advantage that its genome has been sequenced and annotated (Bowes et al. 2010; Hellsten et al. 2010). Our studies began with mature oocytes of *X. tropicalis*, which have a diameter of 800 μm and contain a single, slightly ovoid nucleus, also called the germinal vesicle (GV), with dimensions of about 300 μm x 400 μm (Fig. 1A). In the ovary the oocytes are surrounded by several layers of follicle cells, the most internal of which contains about 1000 cells and is tightly bound to the surface of the oocyte. The follicle layers can be removed completely by treating oocytes with a solution of collagenase (Simeoni et al. 2012). The GV can be isolated from the oocyte by making a small tear in the animal hemisphere with jewelers' forceps and pressing

gently on the sides of the oocyte (Gall and Wu 2010). In many earlier studies, where the major objective was to examine the oocyte lampbrush chromosomes, it was important to prevent gelling of the nucleoplasmic actin (Gall 2006), so that the nuclear contents could be spread in a single plane for microscopical examination (Fig. 1B-D). Here the objective was just the opposite, to find an isolation medium in which the nuclear contents would gel rapidly, but which still allowed clean separation of the GV from the cytoplasm. By trial and error we found that the standard isolation medium adjusted to pH 5.6 - 5.8 serves this purpose. In this medium the nuclear contents gel rapidly, becoming opalescent as viewed by incident illumination, and equally importantly the nuclear envelope swells away from the gelled nuclear contents (Fig. 1E-G). The envelope can then be removed with jewelers' forceps, either intact or in two or three pieces.

The importance of removing the nuclear envelope first became apparent in the course of microarray experiments in which we compared the relative abundance of RNA sequences in cytoplasm and GV samples. In our original samples, prepared from GVs with intact envelopes, there was essentially no difference between the GV and the cytoplasm (Supplemental Fig. S1A). In subsequent experiments, in which the envelope was removed, the GV and cytoplasmic RNA samples showed striking differences (Supplemental Fig. S1B). The ratio of total cytoplasmic RNA to total GV RNA in an oocyte is about 500:1 (1 μg vs. 2 ng, based on recovery). We presume that a small amount of cytoplasm remains tightly associated with the nuclear envelope, even after extensive washing of the isolated GV. Unless the envelope is removed, this cytoplasmic contaminant completely overwhelms the genuine nuclear RNA. Preparation of pure

cytoplasmic RNA presents no problem, because the GV can be removed intact from an oocyte in a few seconds (Fig. 1A).

It has been known for a long time that the majority of newly transcribed RNA in late-stage oocytes consists of pre-rRNA, as originally demonstrated by uridine incorporation experiments (Gall 1966). Moreover, the GV must contain nascent transcripts derived from numerous protein coding genes, as implied by studies on the lampbrush chromosomes (Gall et al. 1983; Callan 1986). Nevertheless, it is not known whether nuclear RNA is rapidly processed and exported, nor which sequences might be stored. To be sure that we did not miss any sequence class, nuclear or cytoplasmic, we did not select for poly $(A)^+$ RNA, nor did we initially remove rRNA or its precursors. This sequencing strategy was wasteful in the sense that most of the sequences were derived from rRNA and its precursors, but we hoped that we would not lose sequences that had unexpected characteristics. In our later analyses, we carried out preliminary selection against rRNA, resulting in considerable increase in read depth, but no change in the patterns for most genes.

*Cytoplasmic mRNA consists primarily of spliced exons*

The mature oocyte stores numerous polyadenylated mRNAs, most of which are not loaded on polysomes and therefore are not being translated. Many of these mRNAs are stored for later use during embryogenesis. A recent deep sequencing study of *X. tropicalis* oocyte RNA identified transcripts from approximately 11,000 genes, differing widely in relative abundance from only a few transcripts per oocyte to many thousands (Simeoni et al. 2012). The read depth in our cytoplasmic samples was lower, primarily

because rRNA was not removed before sequencing, and consequently we identified somewhat fewer transcripts (5000 – 7000 depending on the read depth of the sample).

We examined the cytoplasmic expression profiles for many of the more highly transcribed genes. Typical examples, *nasp* (histone H1-binding protein) and *ccne1* (cyclin E1), are shown in Figs. 2 and 3 respectively. The most obvious feature is that the transcript is represented almost entirely by exonic sequences. The exon-intron boundaries are sharp because the sequence reads are continuous across the entire mRNA, and the number of reads at the ends of the 5' and 3' untranslated regions (UTRs) tapers off, because ends of molecules are systematically under-represented when RNA is fragmented and size-selected before amplification and sequencing. The number of reads within the exons of a given gene also varies, although the patterns are similar between independent experiments. Such variation is commonly seen in deep sequencing data and presumably represents systematic bias at various stages of library production, sequencing, or sequence alignment.

For comparison of relative abundance between samples, we calculated the number of fragments per kilobase of exonic sequence per million reads mapped (FPKM)(Mortazavi et al. 2008). We use the designation $FPKM_{exon}$ to emphasize the exonic origin of the sequences. We analyzed all genes for which there was an $FPKM_{exon}$ score greater than 0 (Supplemental information). Supplemental Fig. S2A compares $FPKM_{exon}$ values for 6675 expressed genes from two samples of cytoplasmic RNA from mature oocytes. $FPKM_{exon}$ values were highly correlated between the two samples ($R = 0.94$). These samples were prepared from different animals, and all steps of sample preparation and sequencing were carried out independently.

*GV RNA contains intronic sequences derived from the majority of transcribed genes*

The most striking feature of GV RNA is the presence of intronic sequences and the nearly complete absence of exonic sequences. For many expressed genes, the nuclear and cytoplasmic patterns are more or less complementary, the peaks in one corresponding to valleys in the other. This pattern is obvious when one examines randomly chosen genes with high cytoplasmic representation, such as *nasp* (Fig. 2) or *ccne1* (Fig. 3). Some introns are represented by single peaks that do not extend all the way to the exon borders, whereas other introns display multiple independent peaks. These patterns are less striking for genes with lower levels of transcription, but most expressed genes have only exonic sequences in the cytoplasm and intronic in the nucleus. It is noteworthy that the intronic sequences in the nucleus do not cross intron/exon borders. Because the intronic sequences in the nucleus are not accompanied by exonic sequences and do not overlap intron/exon junctions, they do not represent parts of unspliced transcripts.

To make more quantitative comparisons of nuclear sequences, we could not use FPKM as usually defined, because it is calculated relative to exonic sequence length. Instead, we used a comparable normalization metric, $FPKM_{intron}$ to describe the abundance of nuclear sequences. We first prepared an annotation file for all introns in the genome, which allowed us to display introns in the genome browser (Fig. 2) and to calculate the abundance of intronic sequence reads (details in Material and Methods). $FPKM_{intron}$ is defined as fragments per kilobase of *intronic* sequence per million reads mapped.

For initial analysis, we examined all of the 6675 transcribed genes identified in the cytoplasmic samples. Of these, 6166 (92.4%) have detectable intronic sequences in the nuclear samples, allowing the calculation of $FPKM_{intron}$ values for almost all transcribed genes. Just like $FPKM_{exon}$ values, $FPKM_{intron}$ values are highly correlated between independent samples, attesting to the reproducibility of the sequencing results (R = 0.94, Supplemental Fig. S2B). Because intronic nuclear sequences exist for almost all transcribed genes, the most parsimonious hypothesis is that they result from processing of primary transcripts. If this is true, then one might expect a correlation between the abundance of intronic and exonic sequences for the same gene. This correlation is shown in Supplemental Figure S2C for the transcribed genes that have $FPKM_{intron}$ values in the nucleus. The correlation is positive with a slope of 1.54, but the spread of values is high (R = 0.55).

Any factor that affects the relative stability of intronic and exonic sequences of specific genes will tend to lower the overall correlation between nuclear and cytoplasmic FPKMs. Later we demonstrate that intronic sequences in the oocyte nucleus are unusually stable, but nevertheless are much less stable than exonic sequences from the same genes. Variations in the relative stability of intronic and exonic sequences could account for much of the scatter in Supplemental Figure S2C. In addition there are computational artifacts that affect the determination of $FPKM_{intron}$ that do not affect $FPKM_{exon}$. For instance, some genes have one or more snoRNAs derived from their introns; snoRNAs often reach very high levels in the nucleus, giving rise to an unusually high $FPKM_{intron}$ / $FPKM_{exon}$ ratio. Short introns (< 200 bp) do not have mapped reads, at least in part because the sequencing protocol used in these experiments did not include

short RNAs. Thus short genes with only one or two short introns tend to have a low $FPKM_{intron}$ / $FPKM_{exon}$ ratio. For unknown reasons, introns longer than about 500 nt are usually not uniformly represented along their length (Fig. 3). As a result, genes with multiple long introns tend to have a low $FPKM_{intron}$ / $FPKM_{exon}$ ratio. In summary, although the correlation between $FPKM_{intron}$ and $FPKM_{exon}$ is not high, we favor the hypothesis that nuclear intronic sequences are derived by processing from primary transcripts, not by independent transcription.

*Nuclear intronic sequences are unusually stable*

Theoretical considerations discussed later make it very likely that the intronic sequences observed in the GV must be very stable, with half-lives of days rather than minutes or hours. To address this issue experimentally, we inhibited transcription and splicing in separate experiments and looked for effects on the RNAseq patterns for nuclear and cytoplasmic RNA.

RNA polymerase II transcription was inhibited with actinomycin D. Oocytes were removed from a mature female and placed in OR2 culture medium. Active transcription in the mature oocytes was verified by examination of the lampbrush chromosomes, which exhibited pronounced transcription loops characteristic of RNA synthesis. Some oocytes were placed in actinomycin D at 20 µg/ml, a concentration that inhibits RNA transcription within 1 hr (reviewed in Callan 1986; Gall and Murphy 1998). Fifteen hours later, cytological examination showed contracted chromosomes without lateral loops, indicating that transcription had ceased. GV and cytoplasmic RNA samples were isolated from the actinomycin-treated oocytes and from control oocytes taken from the

same female. The RNAseq data sets obtained from actinomycin-treated oocytes were very similar to those of the controls, both qualitatively (Fig. 3, top four rows) and quantitatively (Supplemental Fig. S3A, B). We conclude, therefore, that transcripts seen in the GV and cytoplasm are stable for a minimum of about 12-14 hrs.

Splicing was examined by depleting oocytes of the essential splicing factor U2 snRNA. Earlier experiments showed that *Xenopus* oocytes can be depleted of U2 by injecting a specific antisense deoxyoligonucleotide (Pan and Prives 1988). The snRNA is reduced to less than 1% of its original amount within 10-30 min and remains at this level for at least 48 hr (Tsvetkov et al. 1992). Under these conditions splicing does not occur and the normally abundant U2 snRNA is not detectable on the lampbrush chromosome loops by in situ hybridization. However, transcription continues for several days (Tsvetkov et al. 1992).

We injected 250 oocytes with a deoxyoligonucleotide against U2 snRNA and a comparable number with water. Approximately 36-48 hr later we isolated 150 GVs from both the experimental and water-injected oocytes and prepared RNA for sequencing. At the same time we isolated cytoplasmic RNA from both samples. After RNAseq we compared the abundance of U2 snRNA in the two GV samples. In GVs from oligo-injected oocytes, U2 snRNA was reduced to approximately 1% of its original value, demonstrating that the treatment was successful (Supplemental Fig. S4A). Aside from this specific effect of oligonucleotide injection on U2 snRNA, control and injected samples were essentially identical. Individual genes showed the same patterns of GV and cytoplasmic sequences as the controls (Fig. 3, bottom four rows). Furthermore, the relative abundances of sequences in the experimental and control samples were very

similar (Supplemental Fig. S4B, C). It is important to note that buildup of *unspliced* RNA (exons and introns) in the GV was not observed, as might be expected from accumulation of unexported nascent transcripts. As discussed later, the apparent absence of unspliced sequences can be explained by the fact that the GV contains only one set of G2 chromosomes; even though these chromosomes transcribe actively, the absolute amount of new RNA produced by them in two days is undetectable in our experiments. Thus, intronic sequences observed at the end of our experiment must have been present from the beginning.

*Nuclear intronic sequences are processed from primary transcripts*

If the stable intronic sequences result from splicing events at the time of mRNA production, they should derive from the same strand as the mRNA. To test this assumption we carried out RT-PCR experiments on introns from six different genes, using forward or reverse primers alone for the initial reverse transcription step, followed by standard PCR amplification with both primers (Fig. 4A). In each case, the reverse primer at the RT step gave a product of the expected size, whereas the forward primer gave no product. Thus, these intronic sequences are derived from the same strand as the mRNA.

Many of the intronic sequences in the GV appear to span the entire length of smaller introns (those less than about 500 nucleotides), suggesting that they might derive from a single intron lariat either with or without prior debranching. However, longer introns are generally represented by a single peak that does not cover the entire intron or by multiple peaks, often superimposed on a low level across a major portion of

the intron (e.g., Figs. 3 - 5). We carried out RT-PCR experiments to examine the peaks from a few selected genes. First, we examined four cases of single peaks that span most of an intron (Fig. 4B). Although in these examples there are few or no reads that map to the exon-intron junctions, it was important to verify experimentally that the stored intronic sequences are not part of unspliced transcripts. In each case RT-PCR demonstrates that the intronic sequences are not connected to adjacent exonic sequences. Although these experiments do not formally demonstrate that the stable intronic sequences are derived by splicing and subsequent processing of introns from primary transcripts, the data are consistent with that hypothesis.

We also tested whether multiple peaks within an intron represent independent molecules, as opposed to sequencing or mapping artifacts. First, we asked whether peaks and valleys could result from the way repeated sequences are mapped by the alignment program (Supplemental Information). Our analysis suggests that repeated sequences do complicate interpretation of the regions in which they occur, but they do not account for the majority of peaks and valleys (Supplemental Figure S5). We also examined multiple peaks experimentally by asking whether two adjacent peaks in the same intron were part of the same molecule or represented independent fragments (Fig. 5). We could amplify sequences within a peak by RT-PCR, but could not amplify a sequence that extended from one peak to the next. At least for the two examples that we analyzed, the intronic sequences were derived by a process that leads to independent fragments within a single intron.

*Nuclear intronic sequences are less stable than cytoplasmic mRNA*

Because introns and exons are formed in equimolar amounts (and the oocyte is a closed system), the relative abundance of introns and exons in whole oocytes should be a measure of their relative stabilities. We first tried to determine relative abundance by examining RNA derived from intact oocytes (cytoplasm + GV). However, when such RNA was sequenced and displayed on the browser, it appeared almost identical to cytoplasmic RNA (Fig. 6, top two rows). In other words, for a given gene the abundance of intronic sequences in the GV is too low relative to the abundance of exonic sequences in the cytoplasm to be detectable at the read depth of our experiments. Fortunately, certain very abundant RNAs that are limited to the GV can be detected in RNA from whole oocytes. These include various non-coding RNAs, such as snoRNAs, 7SK RNA, and RNase P RNA, as well as a number of unannotated sequences. In principle, one can measure their abundance relative to exons in the whole oocyte sample (Fig. 6, top row) and then measure their abundance relative to introns from the same gene in the GV sample (Fig. 6, third and fourth rows). From these two estimates one can calculate the ratio of introns to exons for a given gene. The calculated molar ratio of GV introns to cytoplasmic exons for 12 genes in the mature oocyte was 0.86% (range: 0.02% – 4.50%) (Fig. 6 and Supplemental Table 2). Two features emerge from these numbers. First, intronic sequences in the nucleus are roughly two orders of magnitude less abundant and therefore less stable than their corresponding exons in the cytoplasm. Exceptions include a few cases like the snoRNAs, which can be as abundant as the exonic sequences of the genes in which they occur. Second, the relative stability of introns to exons varies widely from gene to gene. Some of this variability is due to the difficulty of measuring the abundance of intronic sequences for a

given gene. In addition there are undoubtedly real differences in stability of various mRNAs in the cytoplasm and their corresponding introns in the nucleus.

*Intronic sequences are stable during maturation and early cleavage stages*

To determine whether the intronic sequences detected in GVs from mature oocytes persist through oocyte maturation and early development, we sequenced RNA from three developmental stages: oocytes treated with progesterone to induce GV breakdown, 4-8 cell embryos, and mid-blastulae (at which time zygotic transcription begins in *Xenopus*). The RNA profiles from these three samples were essentially identical to each other and to total RNA from mature oocytes (Supplemental Fig. S6). As expected, intronic sequences were not in general detectable in these samples on the genome browser, although snoRNAs and other highly abundant nuclear RNAs could be seen. We therefore designed primers to look for individual introns by RT-PCR, choosing genes whose transcripts are abundant in the mature oocyte. We could easily detect introns in total RNA from progesterone treated oocytes (after GV breakdown), 4-8 cell embryos, and blastulae (Fig. 7). Because there is no transcription during early cleavage stages of *Xenopus* (reviewed in Davidson 1986), we conclude that introns detectable up to the blastula stage must be derived from the stable introns produced by the oocyte.

## Discussion

The major finding of this study is that the GV of *X. tropicalis* stores stable intronic sequences derived from a majority of its transcribed genes. We refer to these as “intronic sequences” rather than introns, because the stored sequences can be

considerably shorter than the entire intron from which they are derived. A few specific examples of stable intronic sequences have been described before (Michaeli et al. 1988; Kopczynski and Muskavitch 1992; Qian et al. 1992; Yang et al. 2011), but these have been considered exceptional. To our knowledge, stable intronic sequences derived from a majority of the transcribed genes in the genome have not been previously described. These sequences from the oocyte nucleus constitute a previously undetected class of non-coding RNA, for which we propose the name stable intronic sequence (sis) RNA.

Stability of sisRNA in the GV was tested by treating oocytes with actinomycin D to inhibit transcription, or with an antisense deoxyoligonucleotide to inhibit splicing. Because both treatments prevent the generation of new introns by splicing, the existence of intronic sequences at the end of the experiment implies that these sequences are stable for at least one or two days. For technical reasons we could not examine total nuclear RNA from developmental stages after GV breakdown. Nevertheless, we could amplify intronic sequences from selected genes by RT-PCR in RNA samples from progesterone treated oocytes (after GV breakdown), 4-8 cell embryos, and blastulae. It is probable, therefore, that sisRNA from the mature oocyte persists during the early stages of embryonic development, at least until zygotic transcription begins at the blastula stage.

Although sisRNA sequences are almost certainly generated by processing from primary transcripts, they occur at a low molar ratio compared to their cognate exons, on the order of 1%. Experimentally this feature is evident from examination of RNA from intact oocytes; that is, oocytes from which the GV has not been removed. An intact

oocyte contains one GV's worth of intronic sequences and one cytoplasm's worth of exons, yet the intronic sequences in such a sample are not detectable at the read depth obtained in our sequencing experiments (Fig. 6). Thus, although the intronic sequences are stable for at least two days, they are considerably less stable than the mRNA stored in the oocyte cytoplasm.

The biological significance of this relationship is best understood in terms of two features that dominate the transcriptional profile of the amphibian oocyte. First, the volume of cytoplasm in a mature oocyte is roughly $10^5$ -$10^6$ that of a somatic cell, yet the absolute concentration of rRNA and of various mRNAs is not unusual (Simeoni et al. 2012; for earlier references, see Davidson, 1986). Second, the GV, as enormous as it is relative to a somatic nucleus, contains only the normal complement of G2 chromosomes, which must produce all the mRNA of the oocyte. In other words, an amphibian oocyte synthesizes and stores orders of magnitude more mRNA than a typical somatic cell, but it does this with a single G2 nucleus. The strategy that accomplishes this extraordinary feat has three essential components. First, the rate of transcription is unusually high; second, transcription continues for weeks or months; and third, the mRNA that is produced is extremely stable. Estimates suggest that the mRNA of *X. laevis*, a close relative of *X. tropicalis*, has a half-life of about 35 days (Davidson 1986), based on earlier experiments of Anderson and Smith (1978) and Dolecki and Smith (1979). Even so, the lampbrush chromosomes in the GV must transcribe at an unusually high rate to produce this much mRNA (Callan 1986). If the intronic sequences in the GV were as stable as the mRNA in the cytoplasm, the GV would accumulate,

over the long period of oogenesis, $10^5$ to $10^6$ more introns than exist at steady state in a typical somatic nucleus. Thus, even though the molar ratio of nuclear intronic sequences to cytoplasmic exons is only about 1%, the absolute number of intronic sequences in the GV is very large.

Introns were discovered 35 years ago (Berget et al. 1977; Chow et al. 1977), and since then much has been learned about the molecular biology of splicing (Hoskins and Moore 2012) and the importance of introns for alternative splicing and the generation of protein diversity (Black 2003). The evolutionary origin and significance of introns has also been extensively studied (Rodriguez-Trelles et al. 2006; William Roy and Gilbert 2006). In addition, some introns are known to be precursors of specific molecules, of which snoRNAs and scaRNA are well-studied examples (Maxwell and Fournier 1995; Kiss et al. 2010). But intronic sequences in general are thought to degrade rapidly after splicing from the primary transcript, and so there has been little reason to suppose that they play significant biological roles. The discovery of sisRNA in the oocyte nucleus now brings that assumption into question and raises a number of new issues. Certain questions can be addressed fairly directly, based on existing techniques. How are sisRNAs processed from the primary transcripts? Are they formed by a specific trimming mechanism after conventional lariat formation and debranching? When and where do these processes occur in the nucleus and where are the final sisRNAs stored? Are sisRNAs associated with specific proteins? The *Xenopus* oocyte, with its abundance of sisRNA, offers a useful system in which to examine these specific molecular issues.

A bigger challenge will be to determine the biological function(s) of sisRNAs. Do they play a major role during oogenesis, or are they synthesized and stored in the GV primarily for use during later embryogenesis? Do they occur in other cell types? Although the ability to obtain pure nuclear and cytoplasmic RNA fractions makes the *Xenopus* oocyte unique for molecular studies, the difficulty of doing genetics on frogs is a serious drawback for functional analysis. We are currently trying to identify sisRNAs in *Drosophila*, where the wealth of genetic tools would make the search for biological function more feasible. Because the oocyte nucleus of *Drosophila* is transcriptionally silent, sisRNAs, if they exist, are likely to be derived from the nurse cells. Despite the technical challenges, it should be possible to enrich for RNA from nurse cell nuclei and determine whether the *Drosophila* oocyte, like that of *Xenopus*, stores sisRNAs and transmits them to the embryo.

## Materials and Methods

### *Animals and oocytes*

Adult female *Xenopus tropicalis* were purchased from Xenopus 1 (Dexter, MI). Animals were anesthetized with 0.15 % tricaine methane sulfonate and one or both ovaries were removed surgically. Pieces of ovary were placed in OR2 medium (Wallace et al. 1973) at room temperature, where the oocytes maintain normal morphology and biochemical properties for several days. For removal of follicle cells, oocytes were treated with collagenase (Liberase, Roche Applied Science) with gentle swirling in plastic culture dishes for 2-3 hours (Simeoni et al. 2012) . The absence of follicle cells was verified by staining oocytes with DAPI (4',6-diamidino-2-phenylindole) at 1 µg/ml and examining at

low magnification with a fluorescence microscope (10X objective). Transcription was inhibited by incubating pieces of ovary in actinomycin D (20 µg/ml) in OR2 medium. Splicing was inhibited by injecting individual oocytes with a single-stranded deoxyoligonucleotide complementary to part of the U2 snRNA molecule (Tsvetkov et al. 1992).

*Preparation of nuclear and cytoplasmic fractions*

We routinely recover ~1 µg of total RNA per oocyte using standard RNA extraction procedures on batches of 10-50 mature *X. tropicalis* oocytes (whole or enucleated). Using similar conditions on batches of 200-1,000 isolated GVs, we recover 2.1 ng of RNA per GV (average of ten experiments). Because the cytoplasm contains roughly 500 times as much RNA as the GV, even a small amount of cytoplasm adherent to the nuclear envelope seriously compromises the purity of a nuclear RNA sample. For this reason we developed a manual technique for removing the nuclear envelope without losing the contents of the GV. Using jewelers' forceps we isolate GVs in an isotonic saline solution at pH 5.6-5.8 (83 mM KCl, 17 mM NaCl, 6.0 mM $Na_2HPO_4$, 4.0 mM $KH_2PO_4$, 1 mM $MgCl_2$, 1.0 mM dithiothreitol, adjusted to pH 5.6-5.8 with HCl). At this pH the nuclear contents begin to gel within seconds after isolation from the oocyte. Simultaneously, the nuclear envelope swells away from the gelled contents (Fig. 1E-G). The envelope can be removed easily with jewelers' forceps, especially because it adheres to the tips of the forceps. GV contents are collected in batches of 10-20 and transferred to a small vial containing 10 mM sodium citrate, 5 mM EDTA, pH 5.0 for

storage. At least 200 GVs are collected for RNA extraction, equivalent to about 400 ng of total RNA.

For isolation of cytoplasmic RNA, oocytes were transferred from OR2 medium to the same solution used for GV isolation, except at pH 7.0. The GV was removed with jewelers' forceps (Fig. 1A) and the enucleated cytoplasm was transferred in minimal liquid to a 2 ml Eppendorf tube on dry ice.

*RNA extraction*

Defolliculated whole oocytes and enucleated oocytes were frozen singly or in groups of 5-10 in a 2 ml plastic Eppendorf tube on dry ice. Groups of 200-1,000 GVs were collected as described above and stored frozen until used. RNA was extracted in a guanidinium thiocyanate/phenol/chloroform mixture (TRIzol, Ambion) and purified according to the manufacturer's protocol. RNA was quantitated with a NanoDrop 2000 spectrophotometer (Thermo Scientific) and further characterized by electrophoresis in a Bioanalyzer 2100 (Agilent).

*RT-PCR Analysis of Introns*

RT-PCR analysis of selected genes (Supplemental Table 1) was carried out on the same RNA samples that were used for deep sequencing. Total RNA was reverse transcribed for 1 h using AMV-RT (New England Biolabs) and random hexamers. The cDNA was then purified and used for PCR (40 cycles). In Figure 5, Peak 1F and Peak 2R primers gave a product when tested against genomic DNA (gDNA), but not when tested against nuclear RNA (RT+). To demonstrate that these primers are competent

when tested on RNA, we cloned the region spanning Peak 1F through Peak 2R. We then made an *in vitro* RNA transcript from this clone to use as a template in a one-step RT-PCR reaction (Qiagen), which gave a positive PCR product (lanes marked RNA in Fig. 5). For determining strand specificity of selected introns, one-step RT-PCR was used (Qiagen) with a single primer for the reverse transcription step, followed by PCR with both sets of primers (40 cycles). PCR products were visualized on 1% agarose gels.

*Sequencing and sequence analysis*

The RNA was fragmented and a cDNA library was generated by random hexamer priming following the protocol in the Illumina TruSeq RNA Sample Preparation Guide. cDNA prepared from GV and cytoplasmic RNA was approximately 200-500 nt in length. 100 bases were read from one end using the Illumina HiSeq 2000 Sequencer. Reads were aligned to the *X. tropicalis* genome (assembly version 4.1) using the TopHat version 1.2.0 and Bowtie version 0.12.7 sequence alignment programs (Langmead et al. 2009; Trapnell et al. 2009). The Cufflinks program version 0.9.3 (Trapnell et al. 2010) was then used to generate $FPKM_{exon}$ values for the entire genome. To obtain comparable data for introns, it was necessary to generate an intronic gene transfer format (GTF) file for use with Cufflinks. We downloaded exon-intron junction information from XenBase and generated a GTF file that listed the locations of introns rather than exons (Figure 2). Since a typical annotation file lists only the exons of a gene, Cufflinks uses that information to quantify the overall expression levels of the exonic regions ($FPKM_{exon}$). However, given an intronic annotation file, Cufflinks will calculate intronic

expression levels ($FPKM_{intron}$). We used these $FPKM_{intron}$ values to compare intronic data from our various sequencing runs. Sequence alignments were examined in the Integrative Genomics Viewer (IGV) from the Broad Institute (Robinson et al. 2011). Other analyses, especially pair-wise comparisons of RNA from different samples, were carried out with the Spotfire DecisionSite 9.1 analysis software (TIBCO).

*Microarray analysis*

RNA samples were amplified and biotin-labeled according to the Affymetrix manufacturer's 3' IVT Express protocol, hybridized to the Affymetrix GeneChip *Xenopus tropicalis* Genome Array, and scanned in the Affymetrix GeneChip Scanner 3000. Data were extracted and normalized with the Robust Multi-array Average (RMA) in the Partek Genomics Suite 6.5 (Partek, Inc) and analyzed with the Partek and Spotfire platforms.

**Acknowledgments**

We thank Nicholas Ingolia for invaluable help with RNA sequencing and computation, Allison Pinder for extraordinary care in library production and sequencing, and Steven Ching for technical assistance. Microarray analyses were performed by the Johns Hopkins Medical Institutions Deep Sequencing & Microarray Core Facility. Research reported in this publication was supported by the National Institute of General Medical Sciences of the National Institutes of Health under award number R01 GM33397. The content is solely the responsibility of the authors and does not necessarily represent the official views of the National Institutes of Health. JGG is American Cancer Society Professor of Developmental Genetics.

**References**

Anderson DM, Smith LD. 1978. Patterns of synthesis and accumulation of heterogeneous RNA in lampbrush stage oocytes of Xenopus laevis (Daudin). *Dev Biol* **67**: 274-285.

Berget SM, Moore C, Sharp PA. 1977. Spliced segments at the 5' terminus of adenovirus 2 late mRNA. *Proc Natl Acad Sci USA* **74**: 3171-3175.

Black DL. 2003. Mechanisms of alternative pre-messenger RNA splicing. *Annu Rev Biochem* **72**: 291-336.

Bowes JB, Snyder KA, Segerdell E, Jarabek CJ, Azam K, Zorn AM, Vize PD. 2010. Xenbase: gene expression and improved integration. *Nucleic Acids Res* **38**: D607-612.

Callan HG. 1986. *Lampbrush Chromosomes*. Springer-Verlag, Berlin.

Chow LT, Gelinas RE, Broker TR, Roberts RJ. 1977. An amazing sequence arrangement at the 5' ends of adenovirus 2 messenger RNA. *Cell* **12**: 1-8.

Clement JQ, Qian L, Kaplinsky N, Wilkinson MF. 1999. The stability and fate of a spliced intron from vertebrate cells. *RNA* **5**: 206-220.

Davidson EH. 1986. *Gene Activity in Early Development*. Academic Press, Orlando, FL.

Dolecki GJ, Smith LD. 1979. Poly(A)+ RNA metabolism during oogenesis in Xenopus laevis. *Dev Biol* **69**: 217-236.

Gall JG. 1966. Nuclear RNA of the salamander oocyte. In *The Nucleolus - Its Structure and Function National Cancer Institute Monograph 23* (eds. WS Vincent, OL Miller, ME Drets, FA Saez), pp. 475-488. National Cancer Institute, Bethesda, MD.

Gall JG. 2006. Exporting actin. *Nature Cell Biol* **8**: 205-207.

Gall JG, Diaz MO, Stephenson EC, Mahon KA. 1983. The transcription unit of lampbrush chromosomes. In *Gene Structure and Regulation in Development* (eds. S Subtelny, F Kafatos), pp. 137-146. Alan R. Liss, New York.

Gall JG, Murphy C. 1998. Assembly of lampbrush chromosomes from sperm chromatin. *Mol Biol Cell* **9**: 733-747.

Gall JG, Wu Z. 2010. Examining the contents of isolated Xenopus germinal vesicles. *Methods* **51**: 45-51.

Hellsten U, Harland RM, Gilchrist MJ, Hendrix D, Jurka J, Kapitonov V, Ovcharenko I, Putnam NH, Shu S, Taher L et al. 2010. The genome of the Western clawed frog Xenopus tropicalis. *Science* **328**: 633-636.

Hoskins AA, Moore MJ. 2012. The spliceosome: a flexible, reversible macromolecular machine. *Trends Biochem Sci* **37**: 179-188.

Kiss T, Fayet-Lebaron E, Jady BE. 2010. Box H/ACA small ribonucleoproteins. *Mol Cell* **37**: 597-606.

Kopczynski CC, Muskavitch MA. 1992. Introns excised from the Delta primary transcript are localized near sites of Delta transcription. *J Cell Biol* **119**: 503-512.

Langmead B, Trapnell C, Pop M, Salzberg SL. 2009. Ultrafast and memory-efficient alignment of short DNA sequences to the human genome. *Genome Biol* **10**: R25.

Macgregor HC. 1962. The behavior of isolated nuclei. *Exp Cell Res* **26**: 520-525.

Maxwell ES, Fournier MJ. 1995. The small nucleolar RNAs. *Annu Rev Biochem* **35**: 897-934.

Michaeli T, Pan ZQ, Prives C. 1988. An excised SV40 intron accumulates and is stable in Xenopus laevis oocytes. *Genes Dev* **2**: 1012-1020.

Mortazavi A, Williams BA, McCue K, Schaeffer L, Wold B. 2008. Mapping and quantifying mammalian transcriptomes by RNA-Seq. *Nature Methods* **5**: 621-628.

Oesterreich FC, Preibisch S, Neugebauer KM. 2010. Global analysis of nascent RNA reveals transcriptional pausing in terminal exons. *Mol Cell* **40**: 571-581.

Ooi SL, Samarsky DA, Fournier MJ, Boeke JD. 1998. Intronic snoRNA biosynthesis in Saccharomyces cerevisiae depends on the lariat-debranching enzyme: intron length effects and activity of a precursor snoRNA. *RNA* **4**: 1096-1110.

Pan Z-Q, Prives C. 1988. Assembly of functional U1 and U2 human-amphibian hybrid snRNPs in *Xenopus laevis* oocytes. *Science* **241**: 1328-1331.

Petfalski E, Dandekar T, Henry Y, Tollervey D. 1998. Processing of the precursors to small nucleolar RNAs and rRNAs requires common components. *Mol Cell Biol* **18**: 1181-1189.

Qian L, Vu MN, Carter M, Wilkinson MF. 1992. A spliced intron accumulates as a lariat in the nucleus of T cells. *Nucleic Acids Res* **20**: 5345-5350.

Radford HE, Meijer HA, de Moor CH. 2008. Translational control by cytoplasmic polyadenylation in Xenopus oocytes. *Biochim Biophys Acta* **1779**: 217-229.

Richter JD, Lasko P. 2011. Translational control in oocyte development. *Cold Spring Harbor Perspectives in Biology* **3**: a002758.

Robinson JT, Thorvaldsdottir H, Winckler W, Guttman M, Lander ES, Getz G, Mesirov JP. 2011. Integrative genomics viewer. *Nature Biotech* **29**: 24-26.

Rodriguez-Trelles F, Tarrio R, Ayala FJ. 2006. Origins and evolution of spliceosomal introns. *Annu Rev Genet* **40**: 47-76.

Ruskin B, Green MR. 1985. An RNA processing activity that debranches RNA lariats. *Science* **229**: 135-140.

Sharp PA, Konarksa MM, Grabowski PJ, Lamond AI, Marciniak R, Seiler SR. 1987. Splicing of messenger RNA precursors. *Cold Spring Harbor Symp Quant Biol* **52**: 277-285.

Simeoni I, Gilchrist MJ, Garrett N, Armisen J, Gurdon JB. 2012. Widespread transcription in an amphibian oocyte relates to its reprogramming activity on transplanted somatic nuclei. *Stem Cells Dev* **21**: 181-190.

Trapnell C, Pachter L, Salzberg SL. 2009. TopHat: discovering splice junctions with RNA-Seq. *Bioinformatics* **25**: 1105-1111.

Trapnell C, Williams BA, Pertea G, Mortazavi A, Kwan G, van Baren MJ, Salzberg SL, Wold BJ, Pachter L. 2010. Transcript assembly and quantification by RNA-Seq reveals unannotated transcripts and isoform switching during cell differentiation. *Nature Biotech* **28**: 511-515.

Tsvetkov A, Jantsch M, Wu Z, Murphy C, Gall JG. 1992. Transcription on lampbrush chromosome loops in the absence of U2 snRNA. *Mol Biol Cell* **3**: 249-261.

Vargas DY, Shah K, Batish M, Levandoski M, Sinha S, Marras SA, Schedl P, Tyagi S. 2011. Single-molecule imaging of transcriptionally coupled and uncoupled splicing. *Cell* **147**: 1054-1065.

Wahl MC, Will CL, Luhrmann R. 2009. The spliceosome: design principles of a dynamic RNP machine. *Cell* **136**: 701-718.

Wallace RA, Jared DW, Dumont JN, Sega MW. 1973. Protein incorporation by isolated amphibian oocytes: III. Optimum incubation conditions. *J Exp Zool* **184**: 321-333.

William Roy S, Gilbert W. 2006. The evolution of spliceosomal introns: patterns, puzzles and progress. *Nat Rev Genet* **7**: 211-221.

Yang L, Duff MO, Graveley BR, Carmichael GG, Chen LL. 2011. Genomewide characterization of non-polyadenylated RNAs. *Genome Biol* **12**: R16.

**Figure Legends**

**Figure 1.** Isolation of nuclear and cytoplasmic fractions from oocytes of *X. tropicalis*. (*A*) A single mature oocyte of *X. tropicalis* and the GV that was removed from it. (*B-D*) Behavior of GVs isolated at pH 7.0. The nuclear contents form a weak gel after the GV is removed from the oocyte. Such nuclei lose most of their mass, even though the envelope remains intact (Macgregor 1962). The nuclear envelope can be removed (arrow in *D*), but the isolated gel is soft and easily dispersed by pipetting. (*E-G*) Behavior of GVs isolated at pH 5.8. Within a few seconds after isolation the GV becomes opalescent under incident illumination. Then the envelope expands, leaving a wide space between it and the gelled contents. Note that the GV contents do not decrease appreciably in volume. After the envelope is removed (arrow in *G*), the firm nuclear gel can be pipetted without damage. Bars = 500 μm.

**Figure 2**. Cytoplasmic and nuclear sequences from a highly expressed gene, *nasp* (histone H1-binding protein). The predicted exonic and intronic sequences are shown just above the gene name. Solid bars with connecting lines represent the annotated exons (xenTro2). Unconnected solid bars represent introns (see Materials and Methods

for construction of the intron map). The ordinate shows number of reads per base. Cytoplasmic sequences in the lower panel appear as typical spliced mRNA. The exon boundaries are sharp, except for the tapering 5' and 3' ends. The peaks and valleys within the exons presumably reflect systematic biases in library production, sequencing, or sequence alignments; they are more or less reproducible between independent samples. Nuclear sequences in the upper panel are predominately intronic in origin. Conspicuously absent are nascent transcripts, which would be represented by reads along the entire length of the transcribed region. Note the peaks and valleys in the introns, which are reproducible between samples. Some may be artifacts of sequencing, as in the exons, but some of the more prominent peaks probably reflect separate intronic molecules (see Figs 4 and 5).

**Figure 3**. Nuclear and cytoplasmic RNA sequences are stable for at least 2 days. Shown here are patterns for a typical highly expressed gene, *ccne1* (cyclin E1). The ordinates show number of reads per base. *(A)* Actinomycin D Treatment (first four rows). Oocytes were held for 15-16 h in control OR2 medium or in actinomycin D (20 µg/ml) to inhibit transcription. The patterns for GV RNA from control and treated oocytes were essentially identical (1$^{st}$ and 2$^{nd}$ rows). The same was true for cytoplasmic RNA (3$^{rd}$ and 4$^{th}$ rows). *(B)* U2 snRNA depletion (lower four rows). Oocytes were injected with an antisense deoxyoligonucleotide that rapidly destroys U2 snRNA and therefore inhibits splicing. Control oocytes were injected with water. 36-48 h later, RNA was isolated from GVs and cytoplasm from injected and control oocytes. The patterns for GV RNA were similar for control and U2-depleted oocytes (5$^{th}$ and 6$^{th}$ rows). The same was true for cytoplasmic RNA from control and U2-depleted oocytes (7$^{th}$ and 8$^{th}$ rows).

**Figure 4.** Stable intronic sequences are transcribed from the coding strand but are not part of a nascent transcript. *(A)* Intronic sequences in GV RNA could be amplified by RT-PCR only when the RT primer recognized the sense strand. Shown here are the RT-PCR results from amplifying the sense and antisense strands for six genes (cropped in each case from the same gel). *(B)* Intronic sequences could be amplified with two primers within an intron, but not with one primer in an intron and one in an adjacent exon. At the top of the figure is shown part of the gene model for *calm1* (calmodulin 1) and the primers used for RT-PCR. The ordinate shows number of reads per base. A similar intronic peak was examined for three other genes, *nasp* (histone H1-binding protein), *pcna* (proliferating cell nuclear antigen), and *aldoc* (aldolase C). (The primers and corresponding introns are given in Supplemental Table 1).

**Figure 5.** Multiple peaks within a single intron are derived from separate molecules. RT-PCR primers were designed as shown in the gene models for *e2f3* (E2F transcription factor 3) and *gpbp1/1* (GC-rich promoter binding protein 1-like 1). Products were obtained when both primers were within one intronic peak, but not when one was in one peak and the other in an adjacent peak. The bands labeled “RNA” are controls to demonstrate that Peak 1F and Peak 2R primers work when tested on *in vitro* transcribed RNA (details in Materials and Methods). Primers are given in Supplemental Table 1. The ordinates show number of reads per base.

**Figure 6.** Estimating the relative abundance of cytoplasmic exonic and nuclear intronic sequences from the same gene. The method depends on having a super-abundant, strictly nuclear transcript derived from an intron, such as a snoRNA. Shown here is the 5’ end of *trrap* (transformation/transcription domain-associated protein). The ordinates

show number of reads per base. 1st and 2nd Rows. RNA from whole oocyte (cytoplasm + GV) and from cytoplasm only. The large intronic peak in the second intron in the top row (RNA from whole oocytes) is derived entirely from the GV, as shown by its absence from the second row, which displays cytoplasmic RNA only. Quantitation of the peak in Row 1 shows that it occurs (in the whole oocyte) at roughly 2X the molar concentration of the cytoplasmic exonic peaks. 3rd and 4th Rows. These two rows display the GV sequences from *trrap* on two different scales (maximum of 9390 and 50 reads, respectively). In the 3rd row one sees only the super-abundant peak, because it is roughly 200X higher than the other intronic peaks. Since this super-abundant peak is 2X as abundant as the exons and 200X as abundant as the introns, we can conclude that the exons in the cytoplasm are 100X as abundant as the introns in the GV. Quantitative estimates for 16 such cases are given in Supplemental Table 2.

**Figure 7.** Intronic sequences persist up to the blastula stage of embryogenesis. To test whether intronic sequences are stable after GV breakdown and fertilization, RT-PCR was carried out on total egg RNA from progesterone-matured oocytes, 4-8 cell embryos, and blastulae. Intronic sequences were detected in each case. Primers are given in Supplemental Table 1.

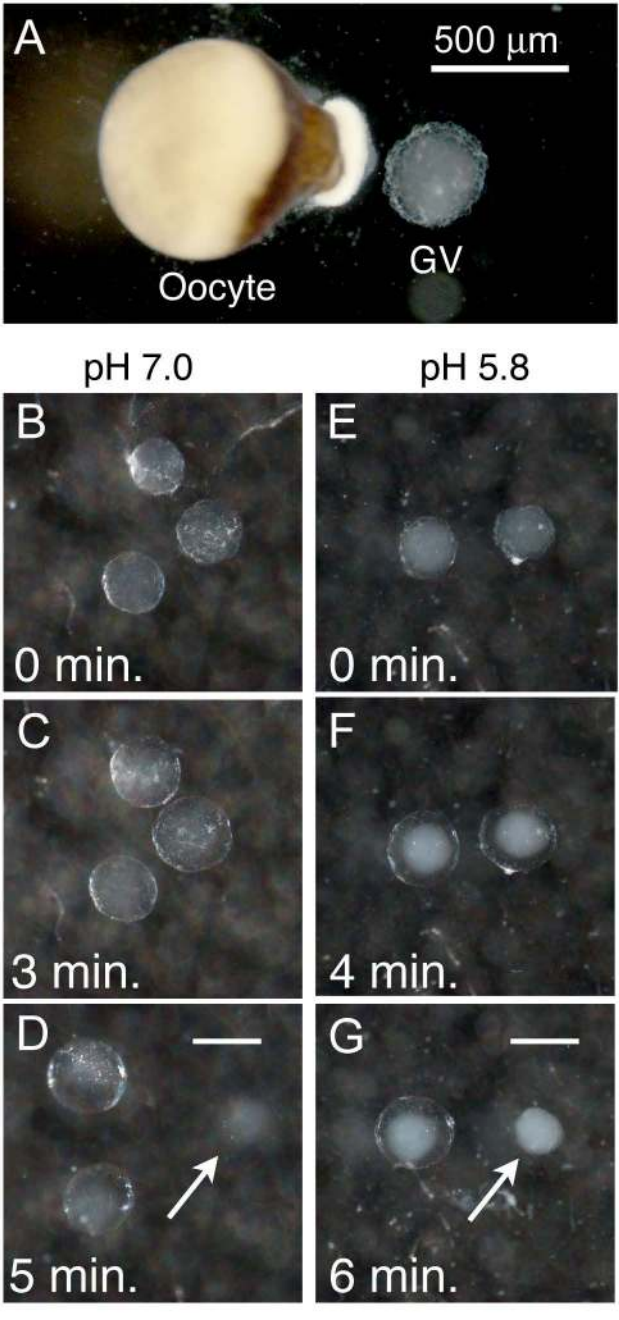
A
500 μm
Oocyte
GV
pH 7.0
pH 5.8
B
0 min.
E
0 min.
C
3 min.
F
4 min.
D
5 min.
G
6 min.

Fig. 2 Gardner et al. GENESDEV/2012/202184

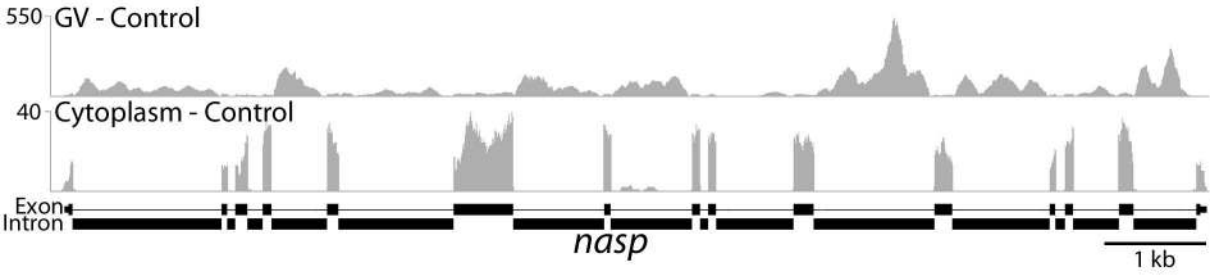

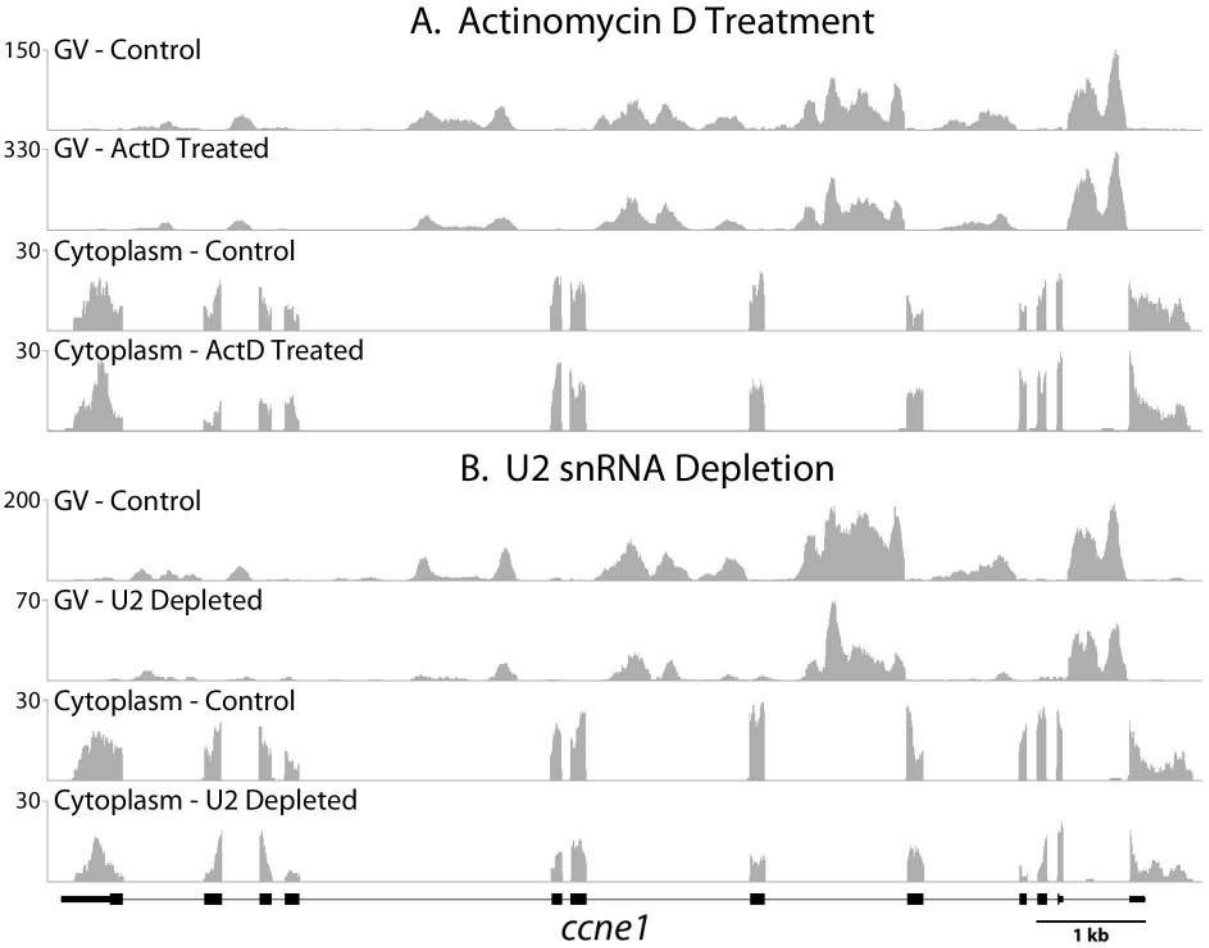
A. Actinomycin D Treatment
150
GV - Control
330
GV - ActD Treated
30
Cytoplasm - Control
30
Cytoplasm - ActD Treated
B. U2 snRNA Depletion
200
GV - Control
70
GV - U2 Depleted
30
Cytoplasm - Control
30
Cytoplasm - U2 Depleted
ccne1
1 kb

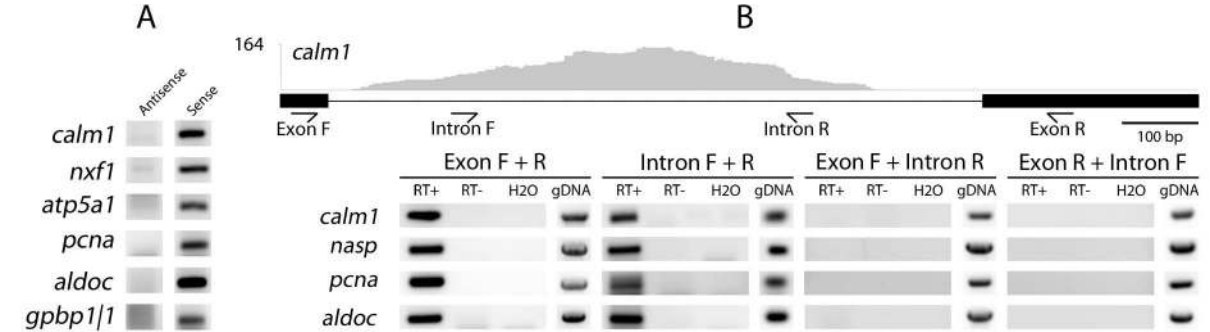
A
Antisense
Sense
calm1
nxf1
atp5a1
pcna
aldoc
gpbp1|1
B
164
calm1
Exon F
Intron F
Intron R
Exon R
100 bp
Exon F + R
Intron F + R
Exon F + Intron R
Exon R + Intron F
RT+
RT-
H2O
gDNA
calm1
nasp
pcna
aldoc

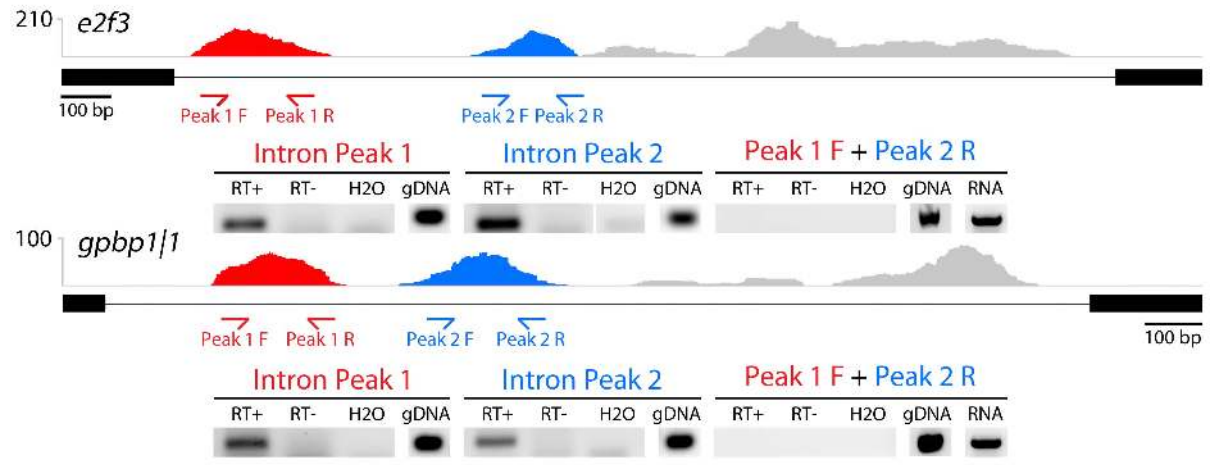
210
e2f3
100 bp
Peak 1 F
Peak 1 R
Peak 2 F
Peak 2 R
Intron Peak 1
Intron Peak 2
Peak 1 F + Peak 2 R
RT+
RT-
H2O
gDNA
RNA
100
gpbp1/1
100 bp

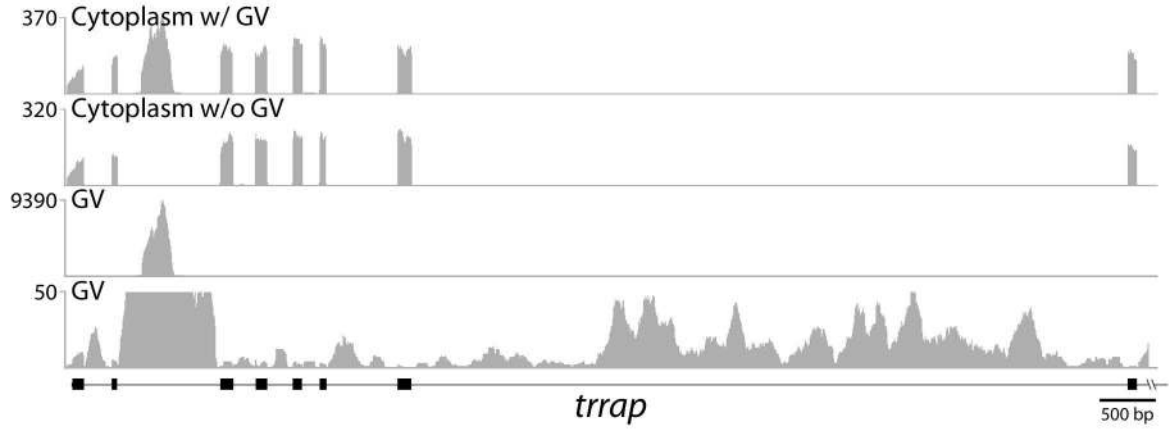
370
Cytoplasm w/ GV
320
Cytoplasm w/o GV
9390
GV
50
GV
trrap
500 bp

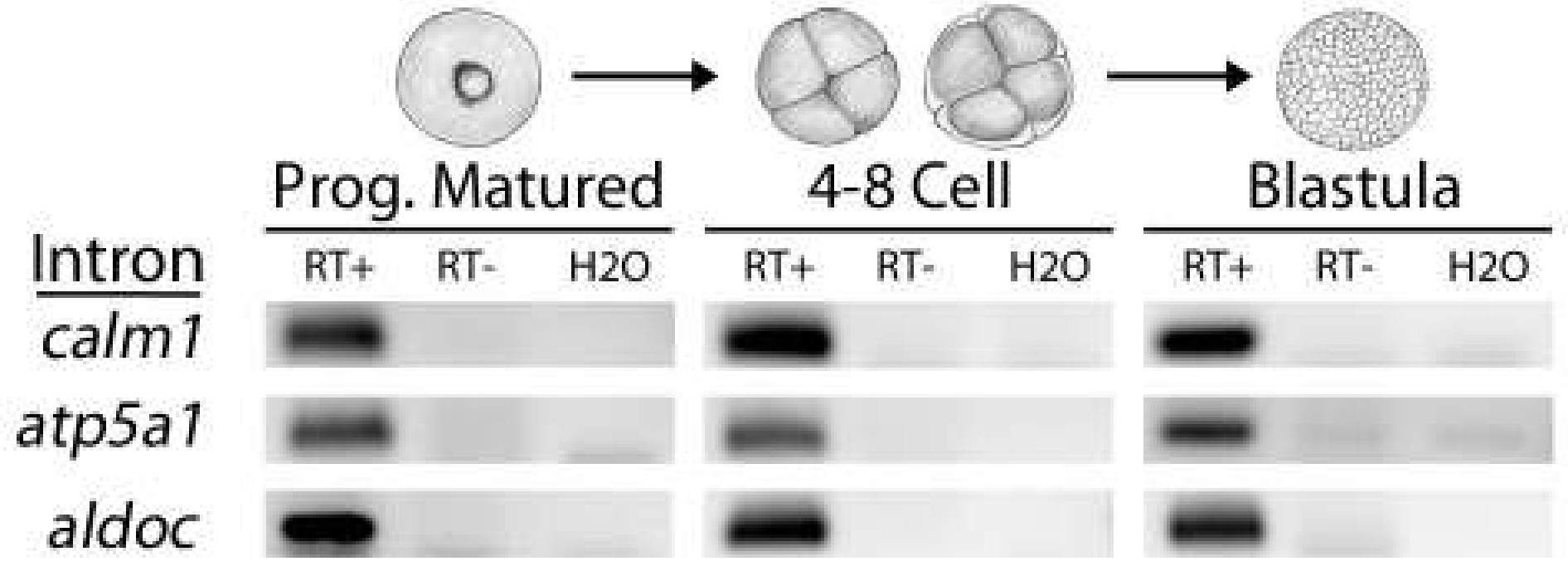
Prog. Matured
4-8 Cell
Blastula
Intron
RT+
RT-
H2O
RT+
RT-
H2O
RT+
RT-
H2O
calm1
atp5a1
aldoc

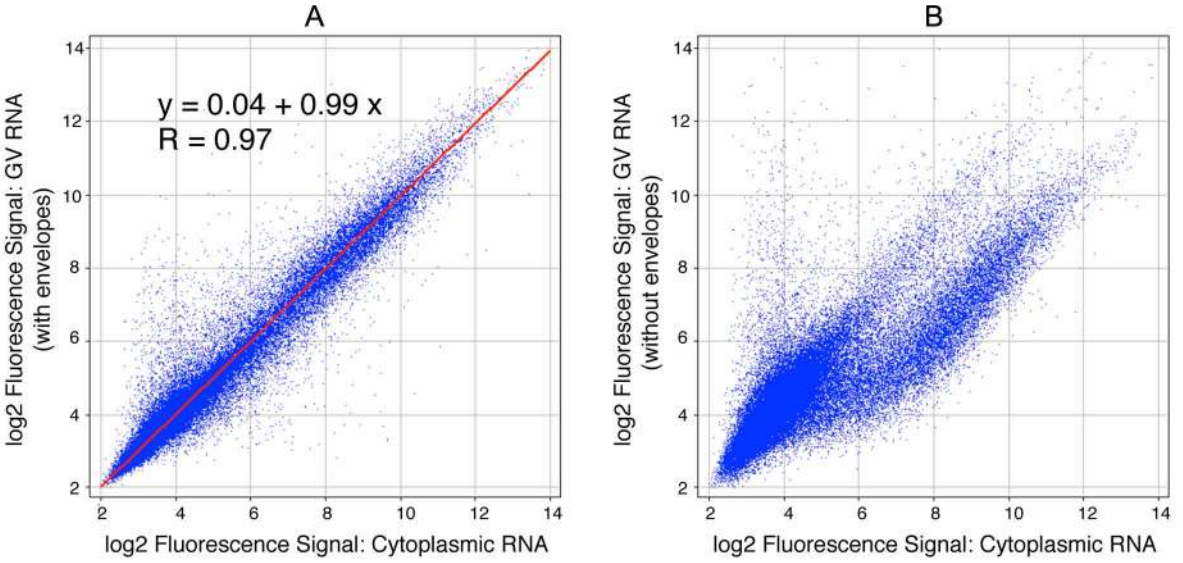
A
y = 0.04 + 0.99 x
R = 0.97
log2 Fluorescence Signal: GV RNA (with envelopes)
log2 Fluorescence Signal: Cytoplasmic RNA
B
log2 Fluorescence Signal: GV RNA (without envelopes)
log2 Fluorescence Signal: Cytoplasmic RNA

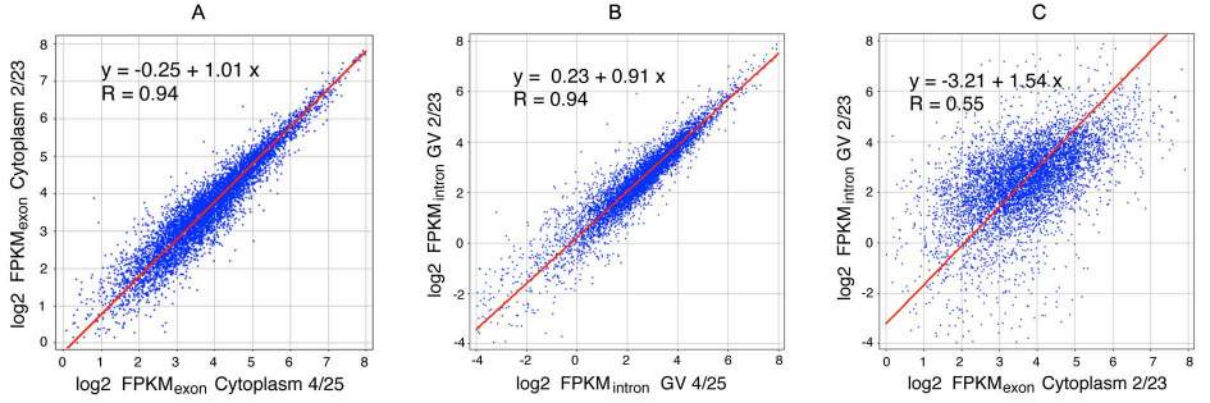
A
y = -0.25 + 1.01 x
R = 0.94
log2 FPKM exon Cytoplasm 2/23
log2 FPKM exon Cytoplasm 4/25
B
y = 0.23 + 0.91 x
R = 0.94
log2 FPKM intron GV 2/23
log2 FPKM intron GV 4/25
C
y = -3.21 + 1.54 x
R = 0.55
log2 FPKM intron GV 2/23
log2 FPKM exon Cytoplasm 2/23

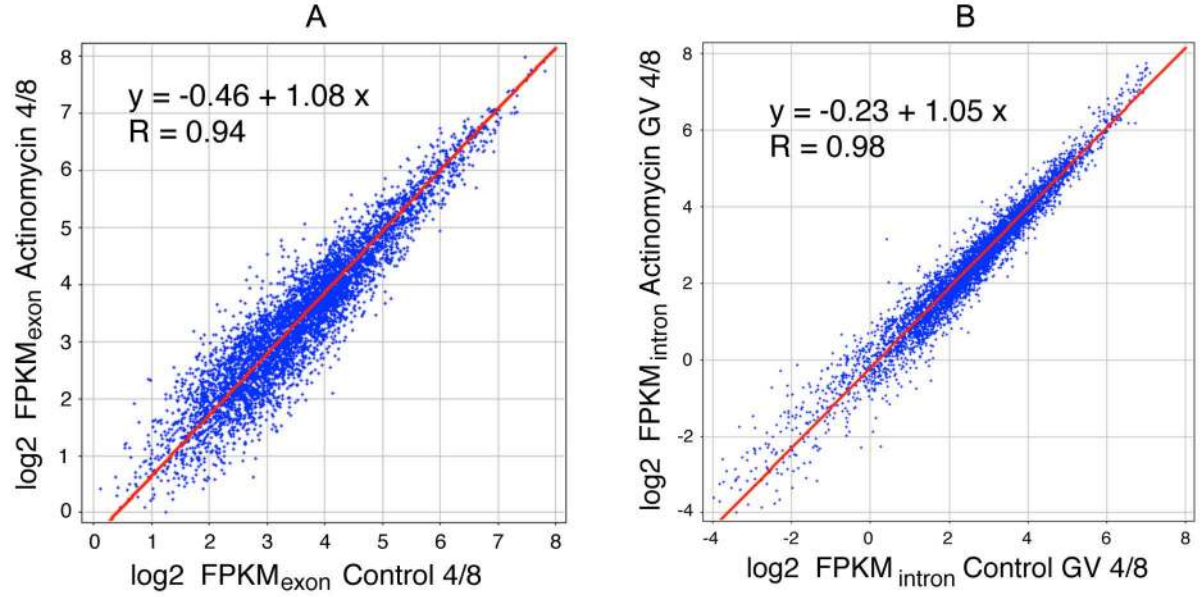
A
y = -0.46 + 1.08 x
R = 0.94
log2 FPKMexon Actinomycin 4/8
log2 FPKMexon Control 4/8
B
y = -0.23 + 1.05 x
R = 0.98
log2 FPKMintron Actinomycin GV 4/8
log2 FPKMintron Control GV 4/8

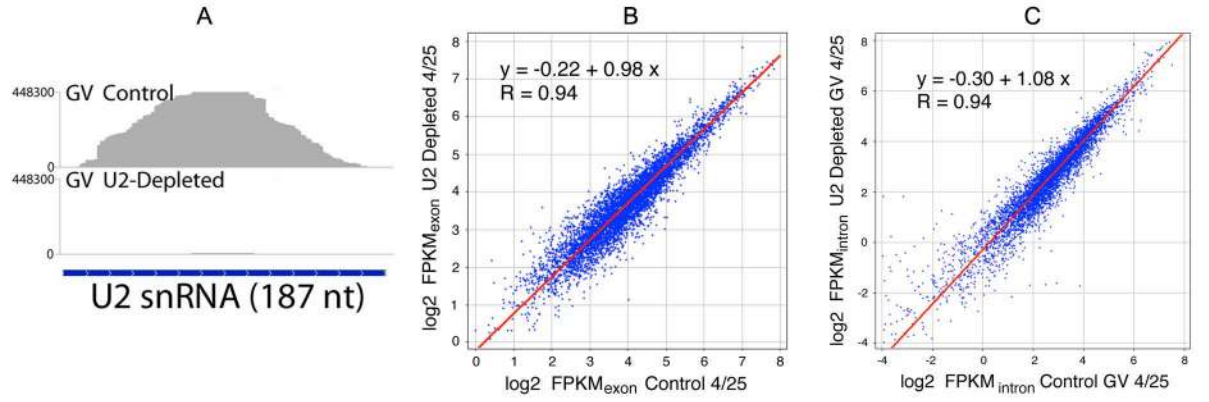
A
448300
GV Control
0
448300
GV U2-Depleted
0
U2 snRNA (187 nt)
B
y = -0.22 + 0.98 x
R = 0.94
log2 FPKMexon U2 Depleted 4/25
log2 FPKMexon Control 4/25
C
y = -0.30 + 1.08 x
R = 0.94
log2 FPKMintron U2 Depleted GV 4/25
log2 FPKMintron Control GV 4/25

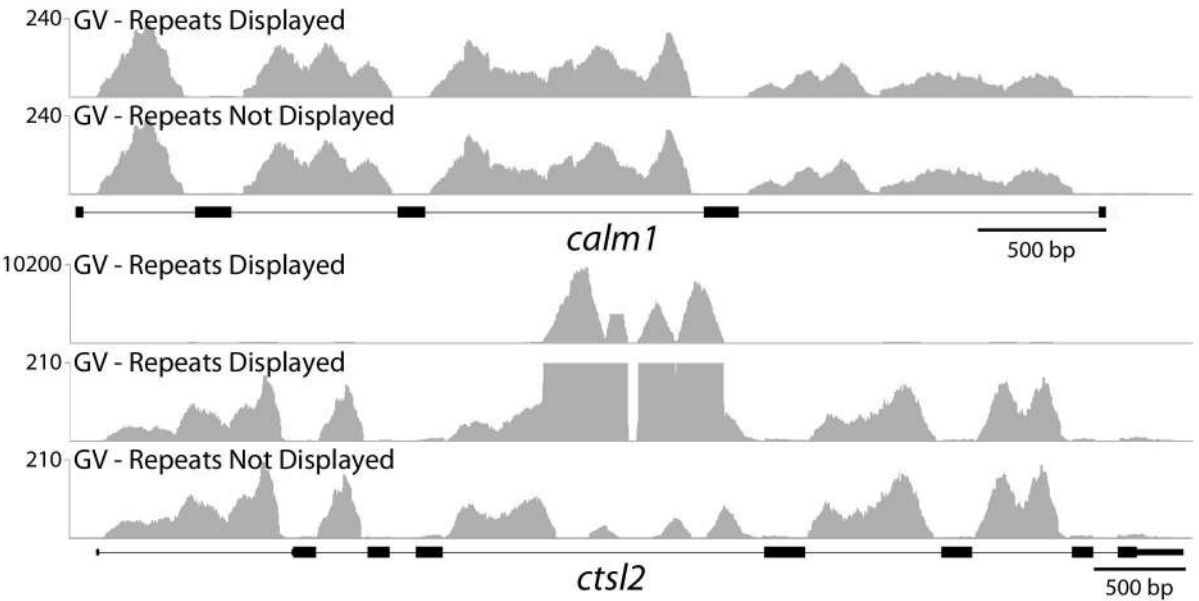
240
GV - Repeats Displayed
240
GV - Repeats Not Displayed
calm1
500 bp
10200
GV - Repeats Displayed
210
GV - Repeats Displayed
210
GV - Repeats Not Displayed
ctsl2
500 bp

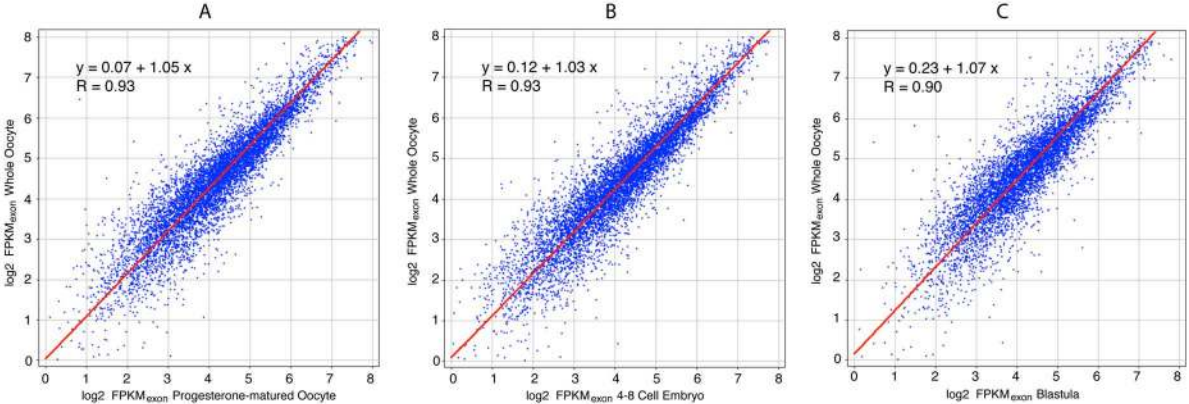
A
y = 0.07 + 1.05 x
R = 0.93
log2 FPKMexon Whole Oocyte
log2 FPKMexon Progesterone-matured Oocyte
B
y = 0.12 + 1.03 x
R = 0.93
log2 FPKMexon Whole Oocyte
log2 FPKMexon 4-8 Cell Embryo
C
y = 0.23 + 1.07 x
R = 0.90
log2 FPKMexon Whole Oocyte
log2 FPKMexon Blastula

# Supplemental Table 1

| | | |
|---|---|---|
| *calm1* | Intron Number 1 | |
| | Exon-F | GCT GAT CAA CTG ACA GAA GAG CAG |
| | Exon-R | TGA AGC TCA GCC TCT GTT GGG T |
| | Intron-F | GGC ATG GAA GTT TGT GTC CAG CG |
| | Intron-R | TGT AAG CAG CAC TGG AGC AGT GA |
| *pcna* | Intron Number 1 | |
| | Exon-F | CGA GCG GCA TCA GCT TGC AG |
| | Exon-R | AGC ATT GTC TTC TGC CCT CAG AGT |
| | Intron-F | GCG CGC AAC CTG GCT TCC C |
| | Intron-R | GCC GCA CTG CTG AAG CTT GG |
| *aldoc* | Intron Number 2 | |
| | Exon-F | AGG GTG ACG AGC GTA TGC AGG A |
| | Exon-R | TGG TGC CAG CAA GAG GGA CC |
| | Intron-F | ACT TGG ATG GTT GCT TAG CTC CCT |
| | Intron-R | CCC CCA GGA CTT TGC AAG CTG T |
| *nasp* | Intron Number 11 | |
| | Exon-F | ACC CAG TCT GTT GGG GTG ATT GA |
| | Exon-R | TGT GGC AGT TGC ATT TTT CTG AGC C |
| | Intron-F | TGG TGG TCC TTG TGA TGG TTC CT |
| | Intron-R | GCC CAC ATC CCA AAG CTA GAG CA |
| *nxf1* | Intron Number 3 | |
| | Intron-F | TCA AGA ACA GGG ATT GCA CTG GGA |
| | Intron-R | TCC TGT CCT ACC TAC GCA TGA TGC |
| *atp5a1* | Intron Number 6 | |
| | Intron-F | GCT TGG TTC TTG GGT TTA TAA |
| | Intron-R | TGT GAA CAG GAC CTT AAA TTG TAA GC |
| *gpbp1\|1* | Intron Number 4 | |
| | Exon-F | ACT GGG GCG CCT ACA GGA GT |
| | Exon-R | AGC TGC TGG TTT AGG GAC CAG A |
| | Peak 1 Intron-F | ACG GCG GGC AAA CCT TTC AGA |
| | Peak 1 Intron-R | GCC GTC GCA CCG AGT ATG AAG C |
| | Peak 2 Intron-F | GCC AAA GCT TTT CAG TGC CCC C |
| | Peak 2 Intron-R | AGT AGT CCA CAC ACA AGC CAA CCA |
| *e2f3* | Intron Number 3 | |
| | Exon-F | CCC GGT ATG ACA CCT CCC TTG GT |
| | Exon-R | TGC CAA GTT GCC TCC ATC ATC AGG |
| | Peak 1 Intron-F | TGC TGA TGC ACC ATG CTA ACC AGT G |
| | Peak 1 Intron-R | TCT TCA GGT ACA CTC TCC AGA TGG C |
| | Peak 2 Intron-F | AAG ATC CCT TAT CCG GAA AAC CCC A |
| | Peak 2 Intron-R | GAG GTG CTG GTA TAC CCA CAG GTT A |

**Supplemental Table 2.**

Relative Abundance of Introns and Exons

| Gene ID | Gene Name (Xenbase) | Intron/Exon |
|---|---|---|
| | | |
| gapdh | glyceraldehyde-3-phosphate dehydrogenase | 0.0022 |
| gapdh | " | 0.0029 |
| slc25a3 | solute carrier family 25, member 3 | 0.0002 |
| atg16/1 | autophagy related 16-like 1 | 0.0069 |
| atg16/1 | " | 0.0104 |
| larp4 | La ribonucleoprotein domain family, member 4 | 0.0174 |
| trrap | transformation/transcription domain-associated protein | 0.0100 |
| timm23 | translocase of inner mitochondrial membrane 23 homolog | 0.0013 |
| timm23 | " | 0.0003 |
| timm23 | " | 0.0024 |
| rps7 | ribosomal protein S7 | 0.0005 |
| eif5 | eukaryotic translation initiation factor 5 | 0.0050 |
| chd9 | chromodomain helicase DNA binding protein 9 | 0.0450 |
| zfr | zinc finger RNA binding protein | 0.0301 |
| ipo7 | importin 7 | 0.0005 |
| tnpo2 | transportin 2 | 0.0017 |
| | | |
| Average | | 0.0086 |

**Supplemental Information**

*Criteria for selection of transcripts to be analyzed*

For the pairwise comparisons of transcripts in Supplemental Figs. S2 – S4 we used the following criteria. From the total set of annotated genes in Xenbase (14,554) we generated a list of all genes in the cytoplasmic samples for which the Cufflinks 0.9.3 program returned an $FPKM_{exon}$ value. Depending on the read depth of the particular sample, this list contained 5,000 – 7,000 genes ("expressed genes"). We then compared two cytoplasmic samples against each other, plotting all genes that had $FPKM_{exon}$ values in both samples (Supplemental Figs. S2A, S3A, and S4B). This process eliminated only a few genes that had low $FPKM_{exon}$ values in one or the other sample. For analysis of nuclear RNA samples, we chose the subset of all expressed genes for which the Cufflinks program returned an $FPKM_{intron}$ value. In three separate experiments this subset contained 92.4%, 94.1%, and 92.4% of the total expressed genes. We did not carry out detailed analysis of "unexpressed" genes, even though this class contained some genes with $FPKM_{intron}$ values.

*Reads from repetitive sequences*

Because of the way repeated sequences are mapped by the Bowtie program (Langmead et al. 2009), repeats in the genome can give rise to spurious valleys in the alignment profile. To test for this possibility we prepared an artificial "genome" consisting of ten genes for which GV RNA showed prominent intronic peaks and valleys. These included the eight genes that we used for RT-PCR analysis of intronic peaks (Figs. 4 and 5; Supplemental Table 1) plus ctsl2 and ccna1. DNA sequences that

occur multiple times in the complete genome are likely to occur only once in such an artificial array. Thus reads will be mapped onto the array that might not map onto the entire genome. Three of the 10 genes in our array contained sequences to which highly abundant GV transcripts mapped. A BLAT search for each of these sequences in the *X. tropicalis* genome revealed that they ranged from 185 - 202 copies per genome. Supplemental Fig. S5 shows the patterns for two genes: *calm1* (calmodulin 1) that does not contain repeated sequences and *ctsl2* (cathepsin L2) that does. Although the repeated sequences in *ctsl2* clearly complicate the interpretation of the short region in which they occur, the majority of the peaks and valleys throughout the introns of these 10 genes are not due to problems with alignment of repeated sequences.

**Supplemental Figure Legends**

**Supplemental Fig. S1.** Microarray analysis of RNA from *X. tropicalis* GVs with and without the nuclear envelope. The log2 value of the fluorescence signal is given on the X and Y axes for individual transcripts. A. Comparison of RNA from oocyte cytoplasm with RNA from GVs that were isolated with the nuclear envelope intact. The two samples are essentially indistinguishable (R = 0.97). B. Comparison of RNA from oocyte cytoplasm with RNA from GVs from which the nuclear envelope had been manually removed. In this case the two samples differ dramatically in the relative abundance of individual transcripts.

**Supplemental Figure S2.** Cytoplasmic and nuclear (GV) RNA from mature *X. tropicalis* oocytes. *(A)* Comparison of log2 $FPKM_{exon}$ values for 6675 genes from two independent samples of cytoplasmic RNA from defolliculated and enucleated oocytes

(800 µm diameter). Results are highly reproducible between independent experiments (R = 0.94). This is the entire population of expressed genes detectable in our experiments *(B)* Comparison of log2 $FPKM_{intron}$ values for 6166 genes from two independent samples of nuclear (GV) RNA from mature oocytes (800 µm diameter). As with the cytoplasm, results are highly reproducible between experiments (R = 0.94). This is the subset of expressed genes that have detectable intronic sequences in the nucleus. *(C)* Comparison of log2 $FPKM_{exon}$ values with log2 $FPKM_{intron}$ values for expressed genes that have detectable intronic sequences in the nucleus. The correlation between cytoplasmic and nuclear values is relatively low (R = 0.55).

**Supplemental Figure S3.** Inhibition of transcription with actinomycin D has little or no detectable effect on transcripts in the cytoplasm and nucleus. Oocytes were held for 15-16 h in control OR2 medium or in actinomycin D (20 µg/ml) to inhibit transcription. Cytoplasmic and nuclear RNA was then isolated and sequenced. *(A)* Comparison of log2 $FPKM_{exon}$ values for cytoplasmic RNA from control and actinomycin-treated oocytes (R = 0.94). Values for 5549 expressed genes were plotted. *(B)* Comparison of log2 $FPKM_{intron}$ values for nuclear (GV) RNA from control and actinomycin D-treated oocytes for the same set of genes (R = 0.98). Values for 5220 genes were plotted. The number of genes is lower than in A because not all genes had $FPKM_{intron}$ values in both samples.

**Supplemental Figure S4.** Inhibition of splicing for 36-48 hr has little or no detectable effect on transcripts in the cytoplasm and nucleus. Oocytes were injected with an antisense deoxyoligonucleotide that causes RNase H-mediated degradation of U2 snRNA within minutes. Control oocytes were injected with water. Cytoplasmic and

nuclear RNA was isolated 36-48 hr later and sequenced. *(A)* Efficient depletion of U2 snRNA is shown by comparing sequence reads from control and oligo-treated oocytes. U2 snRNA is a super-abundant nuclear transcript. *(B)* Comparison of log2 $FPKM_{exon}$ values for cytoplasmic RNA from control and U2-depleted oocytes. Values for 5939 genes are plotted (R = 0.94). *(C)* Comparison of log2 $FPKM_{intron}$ values for nuclear (GV) RNA from control and U2-depleted oocytes for the same set of genes. (R = 0.94). The number of genes plotted (5485) is lower than in B because not all genes had $FPKM_{intron}$ values in both samples.

**Supplemental Figure S5.** Mapping highly repeated sequences onto a small subset of genes. *(A)* Top two rows. Alignment of GV RNA reads for *calm1* (calmodulin 1) to an artificial "genome" of 10 genes (repeats displayed) and to the entire Xentro2 genome (repeats not displayed). The alignments are identical. *(B)* Bottom three rows. Alignment of GV RNA reads for *ctsl2* (cathepsin L2). In the first two rows the reads are aligned to the artificial genome (repeats displayed) but are shown on two different scales. In the bottom row the reads are aligned to the entire Xentro2 genome (repeats not displayed). Repeated sequences that occur in the middle of the largest intron are expressed in the GV, but not necessarily from this particular gene. See Supplemental information for details.

**Supplemental Figure S6.** Transcripts from *(A)* progesterone-matured oocytes, *(B)* 4-8 cell embryos and *(C)* blastulae. In each case deep sequencing was carried out on total cellular RNA. $FPKM_{exon}$ values were compared to values from whole oocyte RNA (defolliculated but not enucleated oocytes). A total of 7267, 7629, and 6111 transcripts were plotted in A, B, and C respectively. The overall similarity of the data for the three

time points is consistent with the known stability of mRNA during early developmental stages of *Xenopus* (R = 0.93, 0.93, and 0.90 in A, B, and C respectively).

**Supplemental Table 1.** Eight genes whose intronic sequences were examined by RT-PCR. The gene names are shown in the first column. The intron examined and specific primers are given in the second and third columns.

**Supplemental Table 2.** Estimation of intron/exon ratio. As shown in Fig. 6, some introns code for highly abundant, strictly nuclear RNAs. These sequences can be detected in RNA derived from whole oocytes but not in RNA from enucleated oocytes. They can also be detected in RNA from GVs. These high-abundance nuclear RNAs can be used to compare the relative abundance of cytoplasmic and nuclear transcripts from the gene in which they occur. The peak height of the special RNA (S) is first determined relative to the peak height of adjacent cytoplasmic exons (E) in the whole oocyte sample (Fig. 6, top row). The peak height of the special RNA (S) is then compared to the peak height of adjacent intronic sequences (I) in the GV sample (Fig. 6, rows 3 and 4). Because the intronic sequences are variable in amount, the ten highest peaks next to the special RNA were averaged to give the intronic peak height (I). The ratio of GV intron to cytoplasmic exon (I/E) was then calculated by multiplying the two fractions (I/S X S/E). Values of I/E for are given in the table. For gapdh, atg16/1, and timm23, there were 2, 2, and 3 special RNAs in separate introns, allowing more than one estimate of the intron/exon ratio.